# Can continuous streamflow data support flood frequency analysis? An alternative to the partial duration series approach

Claps P.* and Laio F.*

*Dipartimento di Idraulica Trasporti e Infrastrutture Civili, Politecnico di Torino, Corso Duca degli Abruzzi, 24, 10129 Torino, Italy.

**Abstract**

Common procedures for flood frequency modeling are based on analysis of series of annual maxima (AMS) of the instantaneous discharge. A practical alternative to AMS series is usually considered when the record length is short. In this case, analysis of Partial Duration Series (PDS) on continuous streamflow records allows one to increase the available information by using more than one flood peak per year. In this paper, the analysis of continuous streamflow data is reconsidered from the beginning: a Filtered Peaks Over Threshold (FPOT) procedure is proposed as an alternative to the PDS approach, and objective criteria are devised for choosing a reasonable threshold and for determining the average annual number of events $\lambda$. The revised procedure demonstrates that there is no need for specific limitations on the magnitude of $\lambda$ to preserve the basic hypotheses of the marked point process build in the PDS procedure. The proposed FPOT method is applied to 33 time series of daily runoff from rivers of North-Western Italy. Significant advantages over the classical PDS method are demonstrated, both in terms of physical interpretability of the parameters and efficiency of the estimates.

Keywords: Floods, PDS Analysis, FPOT Analysis, Extreme Events, Daily runoff.

# 1 Introduction

Management and planning of areas subjected to flood risk heavily relies on tools for flood frequency analysis (FFA), which give the statistical foundations to the planning options. The classical procedure for building at-site or regional flood frequency curves is based on the analysis of annual maxima series (AMS). These series contain the critical information of peak flow amount but their use is limited by two main factors: (i) the length of AMS series can be very short and (ii) AMS series do not have the time continuity that can allow one to infer the state of the basin preceding a given peak. The first limiting factor produces uncertainties in the interpretation of results of purely statistical procedures, while the other point implies that statistical models with phenomenological basis must rely on ancillary data for validation of the underlying hypotheses on the antecedent soil state.

Geomorphoclimatic models for derivation of flood frequency curves, mostly built along the path traced by *Eagleson* [1972], can represent a reasonable compromise between the empirical statistical models for FFA [see e.g. *Bobée et al.*, 1993; *GREHYS*, 1996] and the rising breed of models based on continuous streamflow simulation [e.g. *Hashemi et al.*, 2000; *Cameron et al.*, 2000]. In the physically-consistent derivation of flood frequency curves, the statistical properties of flood peaks are often expressed in terms of frequency of occurrence and intensity of the events. These features are related to the characteristics of the forcing process of precipitation.

As regards the occurrence, Poisson-distributed processes have been widely

used, mainly because of their connections with popular distribution functions of extreme values, that allow one to introduce physically-controllable mechanisms in the variability and shape of the frequency curves [e.g. *Rossi et al.*, 1984]. A recent expression of this tendency is the geomorphoclimatic derivation of the flood frequency curve proposed by *Iacobellis and Fiorentino* [2000], in which a key controlling factor for the flood formation mechanism is the ratio between the average annual number of rainfall and flood events, $\lambda_p$ and $\lambda$ respectively. Both parameters assume a great relevance in FFA, and it becomes important to propose methods for their evaluation, possibly based on continuous data in addition to annual maxima.

In this regard, close examination and, sometimes, validation of models for the occurrence processes are found in the Partial Duration Series (PDS) approach to FFA, where continuous-time data are analyzed to statistically derive flood frequency distributions [see e.g. *Lang et al.*, 1999]. More often than not, the information available is represented by average daily flows, and this partly explains why PDS analysis is not perceived as a real alternative to the analysis of AMS. However, the temporal resolution of available time series is rapidly increasing, thanks to the widespread installation of automatic gauging stations. In any case, even at the daily time scale, the PDS procedure is very useful for obtaining good estimates of $\lambda$.

In actual applications of the PDS method [e.g., *Lang et al.*, 1999; *Robson and Reed*, 1999] values of $\lambda$ are usually kept in the range between 2 and 3 (see Section 5), that contrast to physical and statistical considerations. In fact, in

temperate climates the actual number of discharge peaks per year is usually much higher than 2-3. This can be qualitatively verified by visualizing the daily discharge time series and counting the number per year of major peaks. Other proofs are found in the application of the mentioned geomorphoclimatic models, where $\lambda$ values lower than 5 are shown to be quite unreasonable in terms of rainfall-runoff transformation [*Iacobellis and Fiorentino*, 2000; *De Michele and Salvadori*, 2002]. A last indirect confirmation is given by the results of analyses of series of annual maxima with flood frequency distributions that explicitly include $\lambda$ as a parameter: a typical example is the TCEV distribution [*Rossi et al.*, 1984], extensively used in regional analysis of floods in Italy. *Rossi and Villani* [1994, p. 208] show that estimates of $\lambda$ in homogeneous hydrometric regions in Italy fall in the range 3-15.

Large $\lambda$ values are also advantageous under a statistical viewpoint: it is recognized [e.g. *Madsen et al.*, 1997] that $\lambda = 1.5 - 2$ is usually sufficient to have an advantage towards the AMS estimates in terms of variance of flood quantiles. A further increase of $\lambda$ augments the data in the sample, and further improves the efficiency of the design flood estimates (see Section 5). Incidentally, results from a different field (analysis of wind velocity data) show that optimal estimates are obtained with a number of exceedances of the order of ten per year [*Naess and Clausen*, 2001].

Due to this apparent discrepancy between estimated and expected $\lambda$ values, we believe it is worthwhile to re-evaluate the basis over which the traditional PDS analysis has evolved. This is done in the following section, where an

evolution of the PDS method, named Filtered Peaks Over Threshold (FPOT) is introduced. In Section 3, the building of the Poisson-Pareto model for the peaks over threshold is discussed, and in Section 4 the efficiency of estimation of flood quantile is evaluated. The application to an extensive dataset of daily runoff series in Piemonte (Italy) (Section 5) closes the paper.

## 2 Using Continuous Streamflow Data for FFA

The use of streamflow time series in flood frequency analysis usually follows a three-step approach. In the first step, a procedure is adopted to select, from the continuous time series, those values that can reasonably be considered as peak events. Two selection methods are considered here: the classical PDS approach and a newly proposed procedure. Whatever method is chosen, the continuous stochastic process of daily runoff is transformed into a marked point process defined by the two random variables $n$ (number of peaks per year) and $q$ (magnitude of the peak event).

The second step of the flood analysis is the identification of an appropriate model for the marked point process: usual assumptions are that subsequent peaks are independent, that the number of occurrences $n$ per year is Poisson-distributed, and that the probability density function (pdf) of the flood peaks, $f_Q(q)$, is exponential or Pareto. All of these assumptions will be discussed in detail in Section 3.

The building of an appropriate model for the peak events allows one to derive

a design flood ($T$-year event estimate, where $T$ is the return period in years) that can be expressed as

$$q_T = F_Q^{-1}\left(1 - \frac{1}{\lambda T}\right), \tag{1}$$

where $F_Q^{-1}(\cdot)$ stands for the inverse of the cumulative density function (cdf) of the flood peaks, and $\lambda$ is the expected value of $n$, i.e the mean number of events per year.

The third and last step is model estimation, i.e. the inference of appropriate values for $\lambda$ and the parameters of $F_Q(q)$ based on the available data. An estimate of $q_T$ is so obtained, and the accuracy of the estimation method can be studied.

The mentioned three steps are strictly interconnected: the peak selection procedure should be tuned in order to have the basic model hypotheses met; this affects the dimension of the sample from which the parameters are estimated and, in turn, the accuracy of the estimates. It is therefore crucial for the whole statistical analysis to have an efficient and objective peak selection method.

## 2.1 Peak Selection within the PDS Procedure

In the procedure known as PDS or Peaks Over Threshold (POT) [e.g., *Todorovic*, 1978; *Davison and Smith*, 1990; *Madsen et al.*, 1997; *Lang et al.*, 1999; *Robson and Reed*, 1999] the usual approach to peaks selection consists in retaining only those peaks that exceed a certain threshold value $q_b$. An individual peak is

considered as the portion of the continuous hydrograph that exceeds $q_b$ (see Figure 1a, thresholds $q_{b1}$ and $q_{b2}$), and its magnitude corresponds to the highest discharge in this period. Peaks selection is therefore strictly connected with threshold specification.

A number of methods for selecting meaningful thresholds have been proposed in the literature, either based on physical criteria or on statistical considerations. The idea behind the physical (hydraulic) criteria is that only the hazardous flows are interesting [e.g., *Ashkar and Rousselle*, 1983], and the latter are easily identified by considering a suitably high flood for a specific river section. However, the application of this criterion usually reduces the number of considered floods to a value that is too small for a meaningful statistical analysis. In order to include more peak flows in the analysis, it is therefore necessary to lower the threshold level. All of the other statistical methods attempt to do this, but, so far, it does not seem that objective methods to define $q_b$ have emerged in the vast literature in the field (see for example the discussion in *Lang et al.* [1999]).

The main difficulties in the choice of the threshold derive from the fact that this choice affects the basic model hypotheses, in particular regarding the requirement that subsequent peaks are independent. This produces high threshold values, that reduce the beneficial effects (in terms of variance of estimates) of having several peaks per year. Another limitation of the PDS procedure is that, when the thresholds is low, separate peaks can fall in the same upcrossing portion, so that they are erroneously considered as a unique event (see Figure 1a, threshold $q_{b1}$). This effect can be particularly troublesome when time series

with a strong seasonal component are considered, in which case the whole wet season could turn out to be a unique peak event.

## 2.2 Peak Selection within the FPOT Procedure

To overcome the problems described in the previous Section, the peak selection procedure is revised here. The starting point is again the continuous time series of discharge, sampled at the daily time scale. We propose the following procedure to identify the flood peaks:

(i) The events are identified in correspondence to all the local maxima of the time series (open circles in Figure 1a), and the magnitude of each event is assigned as the absolute ordinate of the maximum. The so-called actual peaks (AP) time series is then obtained (black bars in Figure 1b). It is evident how this procedure tends to identify a great number of peaks: some of them are relevant to the flood frequency analysis while some others (for example those around $t = 50$ days in Figure 1) are false peaks, deriving from the noisy component of the signal. It is thus necessary to filter the AP in order to reduce this noisy component.

(ii) A second sequence of peaks is then obtained [see *Claps et al.*, 2002] by subtracting from the magnitude of the AP events the discharge measured at the first relative minimum preceding the event itself (open squares in Figure 1a). In this manner we obtain a sequence of filtered peaks (FP) (white bars in Figure 1b), representing the discharge increment relative to a base level preceding the event. As such, FP events do not strictly represent the real discharge; rather,

they could approximate the effective rainfall component, i.e. the fraction of rainfall that becomes runoff.

(iii) The last step consists in applying a threshold filter to the FP sequence to retain only the large peaks. The problem of choosing a correct threshold for the analysis, that is crucial for the classical PDS approach, is still present in the FPOT procedure; however, in this case one takes advantage by the fact that the noisy component becomes better recognizable when FP events are considered. In fact, the magnitude of false FP events is always very small, while the same is not true for the AP events (compare Figure 1a and 1b). This allows one to get rid of the noisy component using the standard POT high pass filter. The threshold filter applied to the FP sequence produces an occurrence sample, i.e. a sequence of dates when peaks occur; the magnitude of each peak is then assigned as that of the corresponding AP event. The FP sequence is therefore used only for identifying the false peaks and removing the noisy component, while all the remaining frequency analysis is carried out on the absolute flood magnitudes (AP data).

To complete the procedure, a suitable threshold must be determined: in Section 5 it will be discussed how the removal of the noisy component produces independent Poisson-Pareto samples, and how this can be used as a condition for choosing the appropriate threshold. After that, the identification and estimation of the model can be carried out on the resulting marked point process.

# 3 Building the Marked Point Process Model

The definition of the model basic assumptions discussed in Section 2 is crucial for the whole statistical analysis. It is important to analyze in detail if all of them are essential to the model formulation, and how it is possible to select the peak events such that the necessary hypotheses are met.

## 3.1 Independence between Subsequent Peaks

What is usually considered an essential requirement for any flood frequency analysis is that the selected peak events are mutually independent. It should be noticed, however, that the above hypothesis is not essential in the derivation of Equation (1), that is valid also when subsequent peaks are correlated [*Rosbjerg*, 1985]. However, in the latter case model complexity strongly increases: this explains why the mutual independence of peaks is so often invoked in FFA, even at the expense of artificially reducing the number of considered peaks or compromising some of the other model hypotheses.

For example, one of the commonly used methods aimed at selecting independent peaks consists in fixing the average number of peaks per year, $\lambda$, to a value below 2-3 [see *Todorovic*, 1978]. This method has been criticized for its lack of flexibility, but also the proposed alternatives [*Rosbjerg et al.*, 1992; *Madsen et al*, 1997] tend to limit $\lambda$ to values as low as 2-3 (see Section 5 below). The reduction in the degree of dependence between subsequent peaks is also often achieved by imposing the further requirement that a peak is separated from the previous one by a given number of days (usually 5 days plus the natural

logarithm of the basin area in square miles). Moreover, consecutive peak floods are defined as independent only if the inter-event discharge drops below 75% of the lowest of the two peaks (guidelines from the *US Water Resources Council* [1976]). The use of these restrictions, however, distorts the occurrence distribution and constitute a violation of the basic hypothesis of Poisson distributed events [*Askhar and Rousselle*, 1983].

A question arises here: are these limitations really necessary in order to have independent peaks? From the case study we have analyzed the answer seems to be negative, since very often it is possible to extract samples of peak values with larger values of $\lambda$ and reasonably independent peaks.

A more effective approach to the independency issue is needed: a good alternative could be to start from a very low threshold and move the threshold upwards (so reducing $\lambda$ and increasing the average distance between subsequent peaks) until some independence test is met. A possible variable to be used for a test of independence is the autocorrelation coefficient of subsequent peak values (*Miquel* [1984], cited by *Lang et al.* [1999]), but in this case the test would be effective only for normal or near-normal variates, which is usually not the case for daily or hourly discharges. In contrast, the independence test based on the so called Kendall's $\tau$ does not require hypotheses on the parent population. This test is described in Appendix A and applied within the FPOT approach in Section 5.

## 3.2 Distribution of the Peak Occurrences

A second model hypothesis that is often invoked in the PDS approach (based on asymptotic properties of the exceedances process), concerns the distribution of $n$, the number of peaks per year, that is usually assumed to be Poisson, namely

$$f_N(n) = \frac{e^{-\lambda}\lambda^n}{n!}. \tag{2}$$

Again, it is worth noting that the actual distribution of the occurrences does not affect the validity of Equation (1), since it only involves the mean value of that distribution, $\lambda$ [*Lang et al.*, 1999]. On the other hand, hypotheses of independent and Poisson distributed peaks are essential to relate the cdf of the flood peaks, $F_Q(q)$, to that of the annual maxima, $G_Q(q)$, by means of

$$G_Q(q) = e^{-\lambda(1-F_Q(q))}. \tag{3}$$

When the Poisson assumption needs to be respected, an efficient test is the one proposed by *Cunnane* [1979]: appropriate acceptance limits for the dispersion index $I_d$ (the ratio of the variance to the mean) of Poisson distributed data are easily established [see *Lang et al.*, 1999], and it is then sufficient to verify if the sampling dispersion index lies in the acceptance range (see Section 5).

Apart from the definition of Equation (3), however, the Poisson hypothesis does not seem to be essential when FFA is approached through the PDS method: in fact, the binomial and negative binomial distributions are valid alternatives to the Poisson distribution when one parameter is not sufficient to describe the

whole complexity of the $n$ distribution [see *Lang et al.* 1999]. In those cases, relations analogous to Equation (3) can be derived, with the variance of the $T$-year estimate that increases only slightly despite the added parameter [*Önöz and Bayazit*, 2001].

### 3.3 Distribution of Peak Magnitudes

The last model hypothesis regards the distribution of the magnitude of the selected peaks. A common choice is the Generalized Pareto Distribution (GPD), whose cdf is

$$F_Q(q) = 1 - \left(1 - k\frac{q - q_0}{\alpha}\right)^{\frac{1}{k}}, \tag{4}$$

where $q_0$, $\alpha$ and $k$ are the location, scale, and shape parameters, respectively. The GPD is a versatile distribution [*Choulakian and Stephens*, 2001] which reduces to the exponential distribution when $k = 0$. It can also be interpreted as the limiting distribution of independent excesses over threshold [*Davison and Smith*, 1990; *Cox et al.*, 2002]. Note that $q_0$ could eventually be estimated as a third parameter of the GPD [*Tanaka and Takara*, 2001], but this is not the common choice. In fact, in order to avoid overparametrization it is usual to set $q_0$ as the minimum value of the sample of selected peaks, or directly as the threshold level $q_b$. This latter option cannot be used in the FPOT approach because the threshold is applied to filtered peaks. An additional important property of the GPD is that the corresponding annual maxima distribution, obtained

by substituting Equation (4) into Equation (3), is a generalized extreme value (GEV) distribution.

When Equation (4) is set into Equation (1) the $T$-year flood estimate is obtained as

$$q_T = q_0 + \frac{\alpha}{k}\left[1 - \left(\frac{1}{\lambda T}\right)^k\right]. \tag{5}$$

Several methods have been proposed to verify the adequacy of the GPD hypothesis or to directly select a threshold $q_b$ which produces a good fit to the GPD. For example, *Davison and Smith* [1990] and *Lang et al.* [1999] propose a test for the relation between $q_b$ and the mean excess above threshold, that should approach a straight line when the GPD hypothesis is respected. Other authors [e.g. *Tanaka and Takara*, 2001] prefer to directly test the stability of the quantile estimates, i.e. to select a threshold where little difference in the results would ensue if one would have chosen a slightly higher or lower threshold value. However, in the absence of a clear test for stability, these procedures leave very much to the subjectivity of the user (see the application by *Lang et al.* [1999]).

A further approach has been suggested by *Dupuis* [2000], who proposes to apply an optimal bias robust estimation procedure: a weight between 0 and 1 is assigned to each data point (with a high weight meaning that the GPD model is fitting well) and the threshold is modified until all data points have weights close to 1. The approach is interesting, since it transfers at the level of the weights the problem of finding an appropriate threshold, with the result

that a more objective choice is made possible (in a sense, a similar advantage is given by the FPOT towards a PDS procedure). However, it is necessary to run specific simulations in order to understand when the downweighting indicates a serious lack of fit, and the overall procedure can become very cumbersome and of difficult applicability.

A more efficient alternative is to test the goodness of fit of the GPD: the problem is to find appropriate tests for the situation when the parameters of the distribution are unknown and their estimate is based on the sample of exceedances. In this case the classical goodness-of-fit tests are not distribution-free. Only recently, a specific test for the GPD has been established by *Choulakian and Stephens* [2001], based on Cramer-von Mises and Anderson-Darling statistics (see Appendix B). Preliminary analyses showed that the Cramer-von Mises test demonstrates a greater stability and power over the Anderson-Darling test, probably because in the latter possible discrepancies in the left tail of the distribution are provided with excessive weight.

# 4 Efficiency of the Estimation of the $T$-year Flood

The threshold and peaks selection procedure produces a sample of $N$ peaks in $t$ years, possibly following a Poisson-Pareto model (Section 3). Based on the information contained in this sample, the estimation of the $T$-year flood, $\hat{q_T}$, from Equation (5) can be performed. The usual procedure is to obtain from the sample the estimates $\hat{\lambda}$, $\hat{\alpha}$ and $\hat{k}$ of model parameters, and then to insert these

values into Equation (5) for finding $\hat{q_T}$. Obviously, the nature of $\hat{q_T}$ is related to the type of original data: daily average discharge data allow one to estimate only the daily peak $\hat{q_T}$.

Note that the estimate of $\lambda$ as $\hat{\lambda} = N/t$ is univocal and independent of the estimate of $\alpha$ and $k$, for which the choice of an estimation method must face several options. Commonly used methods for the estimate are Maximum Likelihood, Method of Moments and Probability Weighted Moments [e.g. *Madsen et al.*, 1997], while valid alternatives are represented by the cited optimal bias robust estimation [*Dupuis*, 2000], the De Haan method [e.g. *Naess and Clausen* 2001] or the Generalized Maximum Likelihood method [*Martins and Stedinger*, 2001].

The comparison of different estimation methods is a very delicate problem that goes beyond the scope of the paper: see *Madsen et al.* [1997] or *Martins and Stedinger* [2001] for examples of such comparisons. Preliminary analyses on the dataset used in our application, however, have shown that the choice of the estimation method seems to be of secondary importance with respect to the choice of the peak selection procedure or of the correct truncation level. We therefore decided to concentrate on the latter problems, and to use Maximum Likelihood estimators for $\alpha$ and $k$, obtained with the method reported in *Davison and Smith* [1990].

Once an estimate $\hat{q_T}$ is obtained, a crucial point, also for meaningful comparison with AMS methods, is the measure of the accuracy of the estimate. This is often given as the variance of the $T$-year estimate, $\mathrm{var}(\hat{q_T})$. The variance of

the estimation of $\hat{q_T}$ can be obtained in different ways:

(i) asymptotic formulas, that usually give poor approximations of the actual variance [e.g. *Madsen et al.*, 1997], due to the markedly non-gaussian form of the probability distribution of $\hat{q_T}$. An interesting common feature of such formulas is the fact that $\mathrm{var}(\hat{q_T})$ tends to scale with $1/N$ for all the estimation methods. This fact gives a clear clue of the importance of increasing the size of the available sample.

(ii) Monte Carlo simulations [e.g. *Madsen et al.*, 1997; *Martins and Stedinger*, 2001], that are very effective for comparing estimation methods from simulated data, but have a major drawback in the fact that they require sampling from a known distribution while the actual distribution is unknown (at least regarding the parameter values). Taking the sample parameters as the true values, or even carrying out a nonparametric bootstrap (with the empirical frequency distribution as a reference), does not remove the strong assumption that the finite reference sample is equivalent to the whole population [*Fortin et al.*, 1997].

(iii) Bayesian inference [e.g., *Wood and Rodriguez-Iturbe*, 1975; *Kuczera*, 1999], in which case the estimation itself is bypassed and the probability distribution of $q_T$, intended as a random variable, can be formally written and explicitly computed (see Appendix C). Applications of Bayesian inference in the framework of partial duration series can be found in *Rasmussen and Rosbjerg* [1991] and *Madsen and Rosbjerg* [1997]. This method does not present the problems reported above, since it does not require hypotheses of gaussianity

or uniformity between sample and parent distribution. Moreover, the result of Bayesian inference is much more informative with respect to other methods, since it gives the whole pdf of $q_T$, and not only an estimated value and its variance. The only drawback of the method is a practical one, concerning some numerical difficulties to overcome, due to the necessity to carry out multidimensional numerical integrations.

In order to compare the accuracy of the quantile estimates obtained with the PDS and FPOT procedures, we decided to adopt the Bayesian method. The 90% fiducial limits of $q_T$ (see Appendix C) are used as a measure of the estimation accuracy in Section 5.

# 5 Application

33 time series of daily runoff are analyzed to compare the efficiency of PDS and FPOT methods. Drainage basins are located in the North-West of Italy, in the Piemonte region (about 30000 $Km^2$). The morphology and climate of the Alps influence the majority of basins in the considered group, but some basins are located in a different (Apennine) environment. The basins analyzed cover a variety of climatic and geologic features. As such, this database represents a significant starting point with regard to the analysis of daily runoff time series. We report in Table 1 some characteristic features of the drainage basins and of their daily runoff time series. From Table 1 it can be observed that the drainage areas $A$ range within more than two orders of magnitude; the

average elevations $h_m$ also cover a wide range of values and refer to basins where floods are generated directly from rainfall and to basins where snow and ice melting processes dominate. Record length, $t$, average daily runoff, $\mu_Q$, and the maximum measured instantaneous discharge, $Q_{\max}$, also show a great variability. The amplitude of the dataset allows us to compare significantly the parameters obtained through the PDS and FPOT procedures. In the following of the Section we summarize the main results of the application.

## 5.1 Comparison of Threshold Selection Procedures

The two alternative procedures, PDS and FPOT, are compared using the above-mentioned dataset. The PDS procedure is applied in a classical manner, i.e. by imposing a value to the threshold $q_b$ that, at least in theory, allows the basic model hypotheses to be fulfilled. In particular, it was chosen to select $q_b$ by imposing $q_b = \mu_Q + 3\sigma_Q$ [as suggested by *Rosbjerg et al.*, 1992], where $\sigma_Q$ is the standard deviation of the daily runoff process. The latter method was chosen because (i) it does not leave room for the subjectivity of the user, (ii) it does not disregard the physical properties of the analyzed time series (methods that fix $\lambda$ a priori have this drawback), and (iii) it was extensively applied [*Rosbjerg et al.*, 1992; *Madsen et al.*; 1997].

As for the FPOT approach, an example of application of the procedure is presented in Figure 2, where the threshold is called $s$ (as in Figure 1b) to point out that it does not represent an absolute discharge value. The example demonstrates the effect of a variation in the threshold $s$ on the mean annual

number of occurrences, $\lambda$, and on the test statistics: Kendall's $\tau$ (Appendix A), dispersion index $I_d$ (Section 3.2), and the Cramer - Von Mises $W^2$ (Appendix B).

The statistics $\tau$ and $W^2$ assume very high values for low thresholds and have a rapid decrease as threshold rises. This behavior is common to all the analyzed time series, and it is a clear symptom that, for very low $s$ values, the selected peaks are numerous, mutually correlated (large $\tau$ values), and with a strong noisy component (large $W^2$ values). By increasing $s$, the decrease of the number of selected peaks is quite steep (Figure 2d) and the null hypotheses of independence and GPD of the peaks comes to be verified (the dashed lines, representing the 95% acceptance limits, are downcrossed by the continuous lines representing the test statistics). Note that, as mentioned in Section 2.2, the events we are considering are actual discharge peaks (AP sequence). If FP events were considered, the independence test would be passed at lower thresholds, because the filter partially removes the correlation induced by the base-flow component. However, the estimation of the $T$-year flood would become in this case the sum of the $T$-year FP ordinate and the $T$-year base-flow, thus increasing the overall complexity of the procedure.

The dispersion index of the occurrence process, $I_d$, is scarcely correlated with $s$. Moreover, in most cases the sample value lies inside the 95% acceptance limits for all thresholds. The Poisson distribution is therefore a good approximation of the occurrences distribution, also when $\lambda$ is very high.

The FPOT peak selection procedure is completed by choosing a threshold $s$

that allows the above three tests to be jointly met. Among all the thresholds which fulfil the above three conditions, the lower one is chosen in order to have the higher acceptable $\lambda$ value. In case of Figure 2, a threshold $s = 35$ m$^3$/s is selected, corresponding to $\lambda \cong 6.5$ events per year.

As a further test of the accuracy of the GPD hypothesis, we report in Figure 3 an overall measure of the discrepancy between the sampling and hypothetical frequency curves. The Figure is constructed as follows: for each of the available 33 time series, the selected peaks are ranked, obtaining the order statistics $q_{(j)}$, $j = 1, .., N$. A return period $T_j$ is then assigned to each $q_{(j)}$,

$$T_j = \frac{N}{\lambda(N + 0.5 - j)} \tag{6}$$

where the Hazen plotting position is used to evaluate the empirical frequency curve. $T_j$ defines the abscissa of each point in Figure 3, while the corresponding ordinate represents the relative error between empirical and theoretical frequency curves, namely

$$E_{r,j} = \frac{\hat{q_{T_j}} - q_{(j)}}{q_{(j)}} \cdot 100, \tag{7}$$

where $\hat{q_{T_j}}$ is obtained from Equation (5). The procedure is repeated for the 33 time series to obtain the cloud of points in Figure 3. Note that positive and negative errors are nearly equiprobable, showing that the GPD gives a substantially unbiased fit, also for large return periods. A second important

indication of Figure 3 is that, apart from some outliers, for all the points the relative error lies in the range $\mp 60\%$, showing an overall good fit of the GPD to the data.

## 5.2 Analysis of the Annual Average Number of Floods

We have applied the PDS procedure to the 33 series of our dataset, obtaining estimates of $\lambda$ that are reported in Figure 4 (dashed line). These values fluctuate around $\sim 2$ events per year, consistently with the results usually reported in the literature. Note that the result does not change significantly when different peaks selection procedures are applied within a PDS approach (see for example *Davison and Smith* [1990] or *Lang et al.* [1999]). Much higher values are obtained for most of the series with the FPOT procedure (continuous line in Figure 4). Despite the fact that lower $\lambda$ values are usually obtained with the PDS approach, in two out of 33 cases the Kendall's $\tau$ independence test is not passed by the PDS peaks and the Cramer-von Mises test for the GPD hypothesis is not passed for 8 stations.

It is also interesting to discuss the role played by each of the imposed condition on the definition of $\lambda$ within the FPOT procedure. We have thus reported in Figure 4 (as a dotted line) the $\lambda$ values one had obtained by considering only the independence condition in the selection procedure: for half of the basins the dotted and continuous line coincide, which means that the selection of peaks is principally controlled by the independency requirement. In the other cases it is instead the GPD requirement or, very rarely, the Poisson condition, that

determines the $\lambda$ value. An example of this second situation is given in Figure 2, where a threshold of 25 $m^3/s$ would be sufficient to meet the independency condition, while $s = 35$ $m^3/s$ is necessary in order to respect the Cramer-von Mises test.

### 5.3 Comparison of $T$-year Flood Estimates

The last point regards the efficiency of the $T$-year estimates obtained with the PDS and FPOT methods. The case $T = 100$ years is taken as a reference in the following and the probability distribution of $q_{100}$, $f_{Q_{100}}(q_{100})$ is found by means of Bayesian inference (see Appendix C). An example is reported in Figure 5 for a test station. The pdf's found for the different stations with the FPOT procedure (continuous line) usually have a sharper maximum, and span over a smaller range of $q_{100}$ values with respect to the corresponding PDS estimates. The two pdf's are markedly skewed, due to the heavy right tail of the GPD: for measuring the efficiency of the estimates the 90% fiducial limits are therefore to be preferred to the variance of $q_{100}$ .

We report in Figure 6 the upper and lower 90% fiducial limits, $q_{100}^{\pm}$ (see Appendix C) for the 33 time series, normalized with respect to the maximum likelihood estimate of the 100-year flood, $\hat{q}_{100}$, for facilitating the comparison. In 30 out of 33 cases the FPOT procedure produces a narrower fiducial interval with respect to the PDS procedure, with the distance $q_{100}^{+} - q_{100}^{-}$ reduced of a factor up to 3. $q_{100}^{+}$ undergoes great variations from station to station, ranging from $1.5 \cdot \hat{q}_{100}$ to $8 \cdot \hat{q}_{100}$. This great variability is mainly due to the differences in

the record length $t$ (see Table 1) and to the skewness of the sampling distribution of the flood peaks. A further point of interest is that, even when the FPOT procedure is chosen, the fiducial interval for $T = 100$ years is rather large for some of the stations. This is a well known drawback of the GPD [e.g. *Martins and Stedinger*, 2001], a distribution that accompanies a great versatility to a rather low efficiency of the estimates. Other distributions, or the GPD distribution bounded by imposing a prior distribution to the parameters [*Martins and Stedinger*, 2001], can be more efficient in terms of variance of estimates, but this gain is usually paid with a worst fit and an increase of the bias.

# 6 Conclusions

In flood frequency modeling, the partial duration series procedure is a valid alternative to the usual analysis of annual maximum series. The basic idea is to increase the available information by using more than one flood peak per year. However, in the practical applications ambiguous criteria for peak selection affect the efficiency and the practicality of the method. An evolution of the PDS method, named Filtered Peaks Over Threshold (FPOT) is proposed here, aimed at a more efficient exploitation of the potential that the analysis of continuous streamflow data have for the statistical modeling of floods. Firstly, an objective procedure for peaks identification is introduced, that overcomes some problems arising with the more usual upcrossing method. Secondly, the conditions governing the choice of the threshold are reconsidered, taking into account updated

tests for independence and goodness-of-fit to the common Poisson-Pareto model. This allows us to set objective criteria for threshold definition.

Results obtained analyzing 33 time series of average daily discharge are discussed with regard to the estimate of the mean annual number of flood events, $\lambda$. In the classical PDS method this parameter tends to assume values around 2-3, that are not in agreement with physical and statistical considerations. Additional comparisons are made between PDS and FPOT procedures in terms of efficiency of estimation of flood quantiles. A method based on Bayesian inference is used for obtaining fiducial intervals independently of the parameter estimation procedure. Results obtained for our dataset demonstrate the systematically higher efficiency of the FPOT procedure.

## Appendix A: Kendall's $\tau$ Test of Independence

We summarize here some basic information regarding Kendall's $\tau$ test of independence, referring to *Kendall and Stuart* [1967, pp. 473-83] for a detailed treatment of the argument, and to *Ferguson et al.* [2000] for an application to the detection of serial dependence. Consider a sequence $q_1, ..., q_N$ of peak values selected from the daily discharge time series, and their associated ranks $R_1, ..., R_N$. Kendall's $\tau$ test of independence applied to the detection of first order serial dependence is based on the comparison among the pairs

$$(R_1, R_2), (R_2, R_3), ..., (R_{N-1}, R_N). \tag{8}$$

In particular, Kendall's statistics is defined as

$$\tau = 1 - \frac{4N_d}{(N-1)(N-2)}, \tag{9}$$

where $N_d$ is the number of discordances, i.e the number of pairs $(R_i, R_{i+1})$ and $(R_j, R_{j+1})$ that satisfy either $R_i < R_j$ and $R_{i+1} > R_{j+1}$, or $R_i > R_j$ and $R_{i+1} < R_{j+1}$ [*Ferguson et al.*, 2000]. $N_d$ can be defined as

$$N_d = \sum_{i=1}^{N-1} \sum_{j=1}^{N-1} I[R_i < R_j; R_{i+1} > R_{j+1}], \tag{10}$$

where $I[\cdot]$ represents the indicator function of the set $\{R_i < R_j; R_{i+1} > R_{j+1}\}$, i.e. a function that equals 1 when $R_i < R_j$ and $R_{i+1} > R_{j+1}$, and equals 0 in the reverse case.

Under the null hypothesis of independent subsequent peaks and with $N > 10$, $\tau$ approximates a normal random variable with mean

$$E(\tau) = -\frac{2}{3(N-1)}, \tag{11}$$

and variance

$$\mathrm{var}(\tau) = \frac{20N^3 - 74N^2 + 54N + 148}{45(N-1)^2(N-2)^2}, \tag{12}$$

[*Ferguson et al.*, 2000]. When positive dependence is suspected, the one-sided

95% test based on $\tau$ rejects the null hypothesis of independence when the sample $\tau$ exceeds the critical level $\tau_{0.95}$, defined as

$$\tau_{0.95} = E(\tau) + 1.65\sqrt{\text{var}(\tau)}, \tag{13}$$

where 1.65 is the value of the standardized normal variate with 95% non-exceedance probability.

## Appendix B: The Cramer-von Mises Test

A powerful test that a dataset is compatible with being a random sampling from a given distribution is based on the so called Cramer-von Mises statistics [*D'Agostino and Stephens*, 1986],

$$W^2 = N \int_0^\infty [S(q) - F_Q(q)]\, f_Q(q) \mathrm{d}q, \tag{14}$$

where $S(q)$ is the empirical cdf of the variable $q$. $W^2$ is a measure of the mean square displacement between the empirical and hypothetical cdf's, and it is usually calculated as [*Choulakian and Stephens*, 2001]

$$W^2 = \sum_{i=1}^{N} \left[ F_Q(q_{(i)}) - \frac{2i-1}{2N} \right]^2 + \frac{1}{12N}, \tag{15}$$

where $q_{(i)}$ is the $i$-th order statistics of the empirical sample. When the distribu-

tion parameters are estimated from the sample the test is not distribution-free, i.e. the acceptance limits of the test need being evaluated for each distribution. In particular, when $F_Q(q)$ is a GPD with the parameters estimated by the Maximum Likelihood method, the appropriate acceptance limits of the test for different significance levels are tabled in *Choulakian and Stephens* [2001].

# Appendix C: Bayesian Inference for the Poisson-Pareto model

Bayesian inference lays its foundations upon the idea that parameters should be treated as random variables, whose probability density depends upon the chosen model, possible prior information, and empirical data [*Wood and Rodriguez-Iturbe*, 1975]. Leaving aside the possible availability of prior information, we consider the case when the model is described by Poisson distributed occurrences with associated Pareto distributed marks, and the available data are $q_i$, $i = 1, .., N$, discharge peaks in $t$ years.

The probability distribution of $\lambda$ is obtained by first considering the joint probability, $f(n_1, ..., n_t)$, of having $n_1$ occurrences in the first year, $n_2$ in the second, etc ... Under the hypothesis of independence in the occurrence process, $f(n_1, ..., n_t)$ is obtained from Equation (2) as

$$f(n_1, ..., n_t) = \prod_{i=1}^{t} \frac{e^{-\lambda}\lambda^{n_i}}{n_i!} = e^{-\lambda t}\lambda^N \prod_{i=1}^{t} \frac{1}{n_i!}. \tag{16}$$

$f(n_1, ..., n_t)$ can also be interpreted as the probability distribution of $\lambda$ given that we measured $n_i$ occurrences in the $i$-th year, $i = 1, .., t$ (a multiplication constant is necessary to have a proper pdf). The resulting pdf of $\lambda$ is therefore

$$f_\Lambda(\lambda) = C_1 \lambda^N e^{-\lambda t} \tag{17}$$

where $C_1$ is a constant of integration that makes the integral of $f_\Lambda(\lambda)$ over the whole range of $\lambda$ values equal to one. Equation (17) is a classical result in Bayesian analysis [e.g. *Wood and Rodriguez-Iturbe*, 1975].

A completely analogous procedure can be followed to find the joint distribution of $\alpha$ and $k$ from Equation (4),

$$f_{A,K}(\alpha, k) = C_2 \frac{1}{\alpha^N} \prod_{i=1}^{N} \left(1 - I\left[k > 0; q_i - q_0 > \frac{k}{\alpha}\right]\right) \left(1 - \frac{k(q_i - q_0)}{\alpha}\right)^{\frac{1-k}{k}}, \tag{18}$$

where $C_2$ is a constant of integration with the same role of $C_1$ in Equation (17), and $I[\cdot]$ is the indicator function defined in Appendix A, which is needed for properly taking into account the upper bound of the GPD for $k > 0$. The joint probability of $\lambda$, $\alpha$ and $k$ is simply $f_{\Lambda,A,K}(\lambda, \alpha, k) = f_\Lambda(\lambda) f_{A,K}(\alpha, k)$, since $\lambda$ is independent of the other parameters [e.g. *Madsen et al.*, 1997].

Equation (5) provides a functional relationship between $q_T$ and the parameters $\lambda$, $\alpha$ and $k$. The pdf of $q_T$, $f_{Q_T}(q_T)$ can thus be obtained as a derived distribution of $f_{\Lambda,A,K}(\lambda, \alpha, k)$

$$f_{Q_T}(q_T) = C_1 C_2 \int_0^{\infty} \mathrm{d}\alpha \int_{-\infty}^{\infty} \mathrm{d}k \prod_{i=1}^{N} \left( 1 - I \left[ k > 0, q_i - q_0 > \frac{q_T - q_0}{1 - \left(\frac{1}{\lambda T}\right)^k} \right] \right)$$
$$\left( 1 - \frac{\left(1 - \left(\frac{1}{\lambda T}\right)^k\right)(q_i - q_0)}{q_T - q_0} \right)^{\frac{1-k}{k}} e^{-\lambda t} \left( \frac{\lambda}{q_T - q_0} \right)^N \left( \frac{1 - \left(\frac{1}{\lambda T}\right)^k}{k} \right)^{N-1} \quad (19)$$

The multidimensional integrals in Equation (19) are solved numerically in the Mathematica$^{(R)}$ software using an adaptive Genz-Malik algorithm. The upper and lower 90% fiducial limits for $q_T$, namely $q_T^-$ and $q_T^+$, are finally found from the implicit relations

$$F_{Q_T}(q_T^{\mp}) = \frac{1 \mp 0.9}{2}. \quad (20)$$

## Acknowledgements

This work was carried out under CNR-GNDCI grant 01.01025.PF42. The authors are indebted to Paolo Villani for useful discussions in the definition of the problem.

# References


Ashkar, F. and Rousselle, J., Some remarks on the truncation used in partial flood series models, *Water Resour. Res. 19*(2), 477-480, 1983.

Bobée, G., Cavadias, G., Ashkar, F., Bernier, J., Rasmussen, P., Towards a systematic approach to comparing distribution used in flood frequency analysis, *J. Hydrol. 142*, 121-136, 1993.

Cameron, D., Beven, K. J., Tawn, J. A. and Naden, P., Flood frequency estimation by continuous simulation (with likelihood based uncertainty estimation). *Hydrol. & Earth Syst. Sci., 4*, 23-34, 2000.

Choulakian, V., and Stephens, M.A., Goodness-of-fit tests for the Generalized Pareto Distribution, *Technometrics 43*(4):478-484, 2001.

Claps, P., Laio, F., and Villani, P., Assessment of extreme flood production mechanisms through POT analysis of daily data, *Proc. International Conference on Flood Estimation, Berne*, pp. 75-84, 2002.

Cox, D.R., Isham, V.S., and Northrop, P.J., Floods: some probabilistic and statistical approaches, *Phil. Trans. R. Soc. Lond. A 360*, 1389-1408, 2002.

Cunnane, C., A note on the Poisson assumption in partial duration series models, *Water Resour. Res. 15*(2), 489-494, 1979.

D'Agostino, R.B. and Stephens, A.M., *Goodness-of-fit techniques*, Dekker, New York, 1986.

Davison, A.C. and Smith, R.L., Models for exceedances over high thresholds, *J.R. Statist. Soc. B 52*(3), 393-442, 1990.

De Michele, C, and G. Salvadori, On the derived flood frequency distribution: analytical formulation and the influence of antecedent soil moisture condition, *J. Hydrol. 262*, 245-258, 2002.

Dupuis, D.J., Exceedances over high thresholds: A guide to threshold selection, *Extremes 1*(3), 251-261, 1999.

Eagleson, P.S., Dynamics of flood frequency, *Water Resour. Res. 8*, 878-898, 1972.

Ferguson, T.S., Genest, C. and Hallin, M., Kendall's tau for serial dependence, *Can. J. Stat. 28*, 587-604, 2000.

Fortin, V., Bernier, J., and Bobée, B., Simulation, Bayes, and bootstrap in statistical hydrology, *Water Resour. Res. 33*(3), 439-448, 1997.

Groupe de recherche en hydrologie statistique (GREHYS), Presentation and review of some methods for regional flood frequency analysis, *J. Hydrol. 186*, 63-84, 1996.

Hashemi A.M., Franchini M., O'Connell P.E., Climatic and basin factors affecting the flood frequency curve: Part I - A simple sensitivity analysis based on the continuous simulation approach, *Hydrol. & Earth Syst. Sci., 4*, 463-482, 2000.

Iacobellis, V., and M. Fiorentino, Derived distribution of floods based on the concept of partial area coverage with a climatic appeal, *Water Resour. Res. 36*(2), 469-482, 2000.

Kendall, M.G. and Stuart, A., *The advanced theory of statistics. Vol 2. Inference and relationship*, 2nd edition, Griffin and Co., London, 1967.

Kuczera G., Comprehensive at-site flood frequency analysis using Monte Carlo Bayesian inference, *Water Resour. Res. 35*(5), 1551-1557, 1999.

Lang, M., Ouarda, T.B.M.J., Bobée, B., Towards operational guidelines for over-threshold modeling, *J. Hydrol. 225*, 103-117, 1999.

Madsen, H., and Rosbjerg, D., Generailized least squares and empirical Bayes estimation in regional partial duration series index-flood modeling, *Water Resour. Res 33*(4), 771-781, 1997.

Madsen, H., Rasmussen, P.F., Rosbjerg, D., Comparison of annual maximum series and partial duration series methods for modeling extreme hydrologic events. 1. At-site modeling, *Water Resour. Res 33*(4), 747-757, 1997.

Martins, E.S., and Stedinger J.R., Generalized maximum likelihood Pareto-Poisson estimators for partial duration series, *Water Resour. Res. 37*(10), 2551-2557, 2001.

Miquel, J., *Guide pratique d'estimation des probabilites de crue*, Eyrolles, Paris, 1984.

Naess, A. and Clausen, P.H., Combination of the peaks-over-threshold and bootstrapping methods for extreme value prediction, *Structural Safety 23*, 315-330, 2001.

Önöz, B. and Bayazit, M., Effect of the occurrence process of the peaks over threshold on the flood estimates, *J. Hydrol. 244*, 86-96, 2001.

Rasmussen, P.F., and Rosbjerg, D., Evaluation of risk concepts in partial duration series, *Stochastic Hydrol. Hydraul. 5*(1), 1-16, 1991.

Robson, A. and D. W. Reed, *Flood estimation Handbook. Vol. 3: Statistical*

*procedures for flood frequency estimation*, Institute of Hydrology, Wallingford, UK, 1999.

Rosbjerg, D., Estimation of partial duration series with independent and dependent peak values, *J. Hydrol. 76*, 183-195, 1985.

Rosbjerg, D., Madsen, H. and Rasmussen, P.F., Prediction in partial duration series with generalized Pareto distributed exceedances, *Water Resour. Res. 28*(11), 3001-3010, 1992.

Rossi, F., Fiorentino, M., Versace, P., Two component extreme value distribution for flood frequency analysis, *Water Resour. Res. 20*(7), 847-856, 1984.

Rossi F. and P. Villani, A project for regional analysis of floods in Italy. In: *Coping with Floods*, edited by Rossi G., N. Harmancioglu e V. Yevjevich, pp. 193-218, Kluiwer Academic Publisher, Dordrecht, The Netherlands, 1994.

Tanaka, S. and Takara, K., A study on threshold selection in POT analysis of extreme floods, in *The extremes of the extremes: extraordinary floods*, pp. 299-304, IAHS Publ. no. 271, 2002.

Todorovic, P., Stochastic models of floods, *Water Resour. Res 14*(2), 345-356, 1978.

US Water Resources Council, *Guidelines for determining flood flow frequency*, Bull. 17, Hydrol. Comm. Washington (DC), 1976.

Wood, E.F. and Rodriguez-Iturbe, I., Bayesian inference and decision making for extreme hydrologic events, *Water Resour. Res 11*(4), 533-542, 1975.

# Captions

Table 1. Characteristic features of the 33 drainage basins considered in the application. Drainage area $A$, average elevation $h_m$, record length $t$, average daily discharge $\mu_Q$ and maximum measured daily discharge $Q_{\max}$ are reported for each station.

Figure 1. Example of the PDS and FPOT peak selection procedures: in (a) the continuous discharge time series is reported, along with two possible threshold values $q_{b1}$ and $q_{b2}$. The arrows indicate the selected peaks when the threshold $q_{b2}$ is used, while the open squares and circles correspond to the local minima and maxima of the time series, respectively, to be used in the FPOT analysis. In (b) the AP and FP series are reported as black and white bars, respectively, and the arrows indicate the peaks selected with the threshold $s$.

Figure 2. Example of application of the FPOT procedure. In (a), (b), and (c), the test statistics $\tau$, $I_d$, and $W^2$ are reported as functions of the threshold $s$ (continuous lines), along with the 95% acceptance limits of the tests (dashed lines). In (d) the average number of events per year, $\lambda$, is plotted as a function of $s$.

Figure 3. Relative errors $E_r$ (see Equation (7)) between empirical and GPD frequency curves, plotted versus the return period $T$.

Figure 4. Average number of peaks per year for the 33 stations in the dataset.

Figure 5. Probability distributions of the 100-year flood estimate, $q_{100}$, for station n. 32 (river Borbera at Baracche); the value estimated with Maximum

Likelihood, $\hat{q}_{100}$, and the fiducial intervals are also reported in the upper part of the figure.

Figure 6. 90 % fiducial limits of $q_{100}$ (the 100-year flood estimate) normalized with respect to the Maximum Likelihood estimates, $\hat{q}_{100}$, for the 33 considered stations (the horizontal dotted line with ordinate 1 can be used as a reference for the $\hat{q}_{100}$ value).

| | Name | $A$ [Km$^2$] | $h_m$ [m a.s.l] | $t$ [years] | $\mu_Q$ [m$^3$/s] | $Q_{\max}$ [m$^3$/s] |
|---|---|---|---|---|---|---|
| 1 | Ticino at Bellinzona | 1515 | 1615 | 10 | 62.3 | 808 |
| 2 | Toce at Candoglia | 1532 | 1641 | 21 | 63 | 1400 |
| 3 | Ticino at Sesto Calende (Miorina) | 6599 | 1283 | 26 | 296.3 | 1960 |
| 4 | Mastallone at Ponte Folle | 149 | 1350 | 22 | 7.2 | 484 |
| 5 | Sesia at Campertogno | 170 | 2120 | 7 | 6 | 304 |
| 6 | Sesia at Ponte Aranco | 695 | 1480 | 9 | 28.2 | 1710 |
| 7 | Rutor at Promise | 50 | 2616 | 20 | 2.5 | 15 |
| 8 | Dora Baltea at Aosta | 1840 | 2270 | 10 | 48.4 | 280 |
| 9 | Artanavaz at St. Oyen | 69 | 2206 | 16 | 2.2 | 21 |
| 10 | Ayasse at Champorcher | 42 | 2392 | 22 | 1.7 | 27 |
| 11 | Lys at Gressoney St. Jean | 91 | 2615 | 7 | 3.4 | 31 |
| 12 | Dora Baltea at Tavagnasco | 3313 | 2080 | 21 | 96.4 | 1260 |
| 13 | Orco at Pont Canavese | 617 | 1930 | 29 | 19.2 | 530 |
| 14 | Stura di Lanzo at Lanzo | 582 | 1751 | 32 | 19.3 | 696 |
| 15 | Dora Riparia at Oulx (Ulzio) | 262 | 2169 | 10 | 5.0 | 80 |
| 16 | Dora Riparia at S. Antonino di Susa | 1048 | 1613 | 10 | 18.8 | 139 |
| 17 | Chisone at Soucheres | 94 | 2233 | 12 | 2.7 | 29 |
| 18 | Chisone at Fenestrelle | 155 | 2169 | 8 | 3.1 | 43 |
| 19 | Chisone at S. Martino | 580 | 1751 | 29 | 12.6 | 400 |
| 20 | Po at Crissolo | 37 | 2235 | 28 | 1.5 | 81 |
| 21 | Grana at Monterosso | 102 | 1540 | 32 | 2.6 | 114 |
| 22 | Rio Bagni at Bagni Vinadio | 63 | 2124 | 11 | 2.1 | 58 |
| 23 | Stura di Demonte at Pianche | 181 | 2070 | 14 | 4.6 | 95 |
| 24 | Stura di Demonte at Gaiola | 562 | 1817 | 11 | 16.4 | 141 |
| 25 | Corsaglia at C. Molline | 89 | 1530 | 18 | 2.8 | 69 |
| 26 | Tanaro at Ponte Nava | 148 | 1623 | 31 | 4.8 | 174 |
| 27 | Tanaro at Nucetto | 375 | 1227 | 29 | 10.4 | 461 |
| 28 | Tanaro at Farigliano | 1522 | 938 | 34 | 37.8 | 1490 |
| 29 | Tanaro at Montecastello | 7985 | 663 | 37 | 127.8 | 2690 |
| 30 | Erro at Sassello | 96 | 591 | 16 | 2.7 | 81 |
| 31 | Bormida at Cassine | 1483 | 493 | 12 | 24.0 | 1022 |
| 32 | Borbera at Baracche | 202 | 880 | 14 | 5.3 | 228 |
| 33 | Scrivia at Serravalle | 605 | 695 | 14 | 15.0 | 328 |

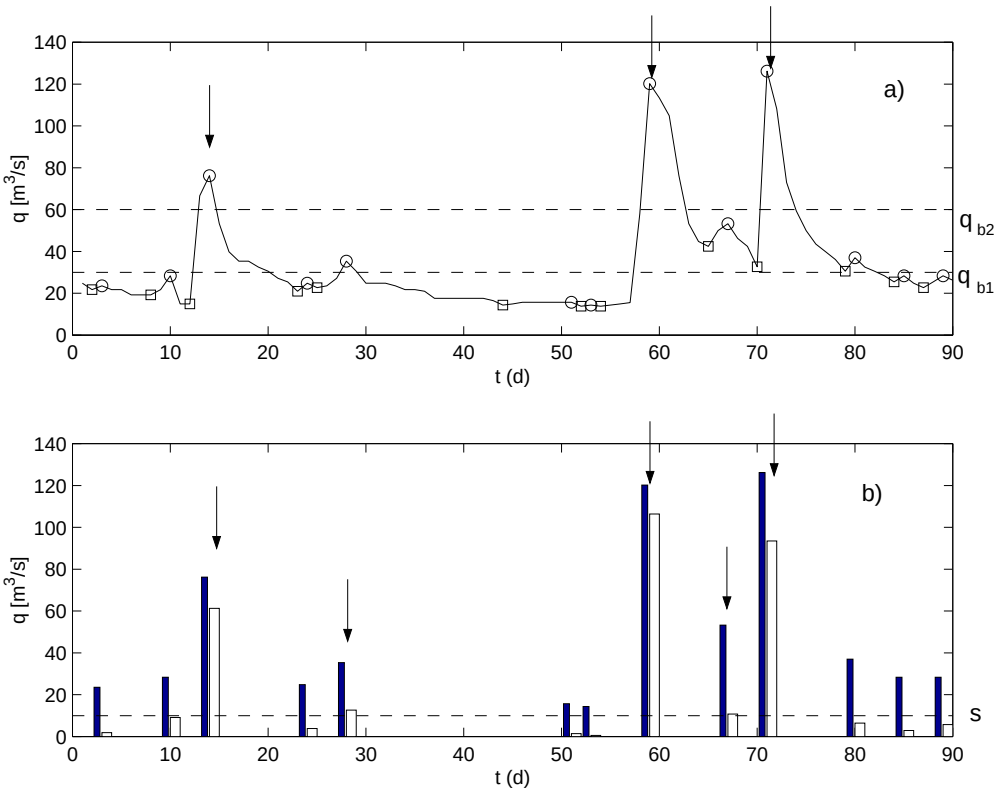


Figure 1: Claps and Laio [2002]

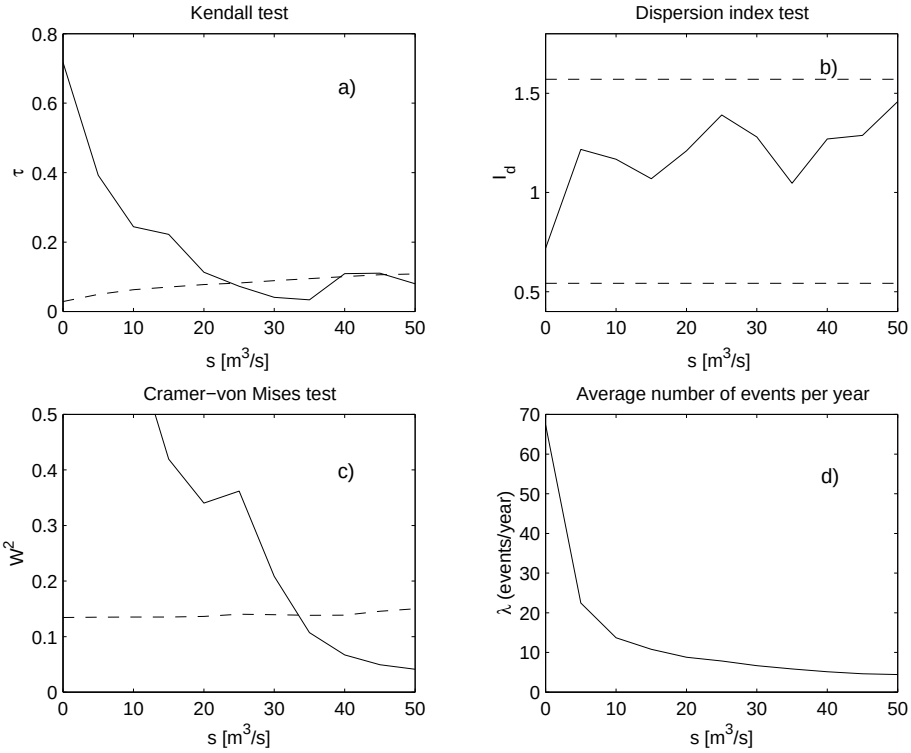


Figure 2: Claps and Laio [2002]

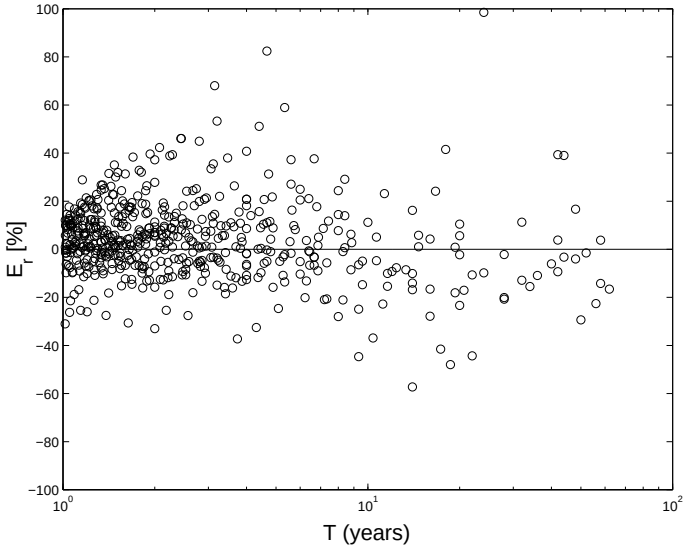


Figure 3: Claps and Laio [2002]

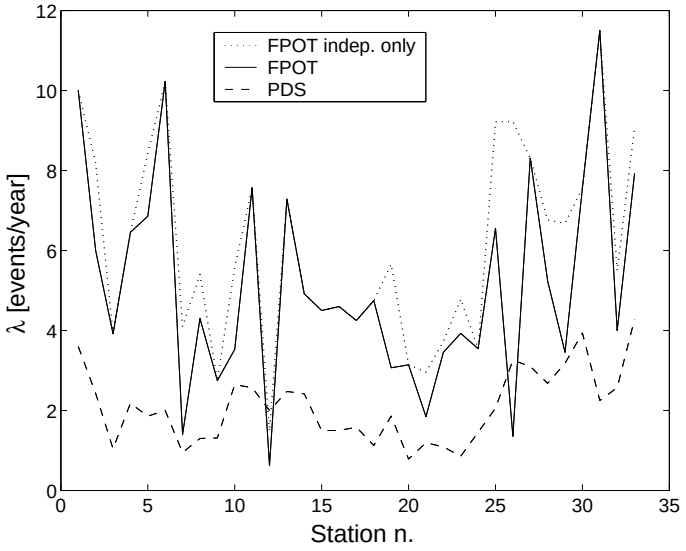


Figure 4: Claps and Laio [2002]

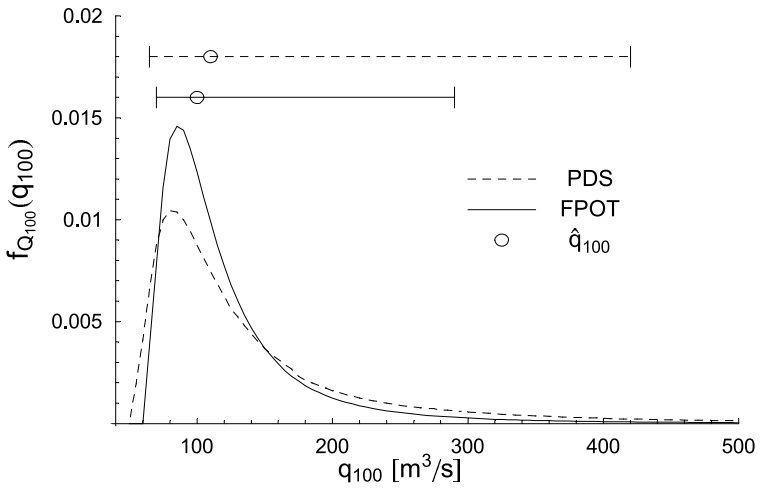


Figure 5: Claps and Laio [2002]

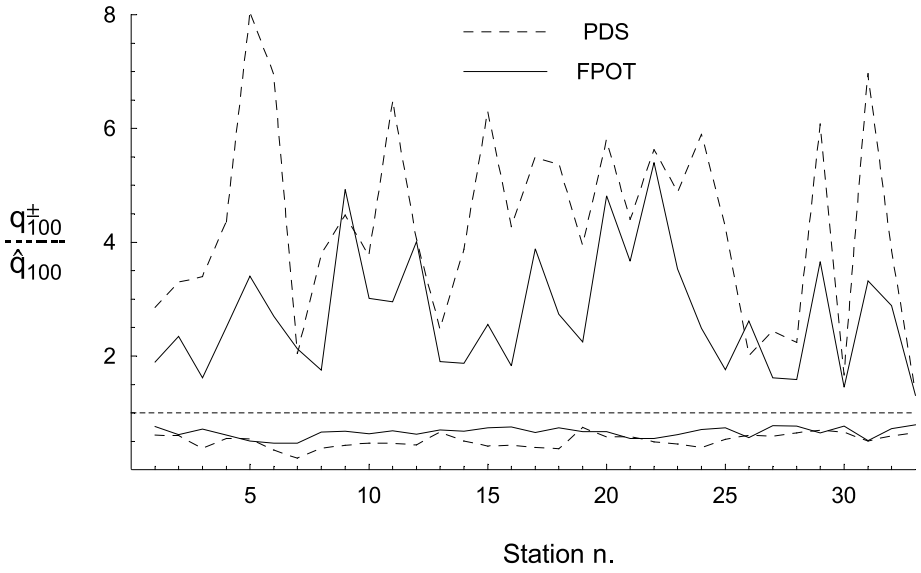


Figure 6: Claps and Laio [2002]